<div align="center">

Supporting information

For

</div>

New synthesis approach for hierarchical MoS$_2$ nanoflakes toward hydrogen evolution in both acidic and alkaline media

Changhai Liu[a], Shengkang Min[a], Yanhua Yao[a], Mohsen Shakouri[b], Lei Zhang[c], Yongfeng Hu[b,*], Zhidong Chen[a,*]

Experimental section

1.1 Chemicals and materials

All chemicals used were analytical reagent grade and used without further purification. Sodium methoxide, thiourea, HCl, KOH, H$_2$SO$_4$ were purchased from Aladdin–Holdings Group. Nafion (5wt%) and multiple carbon nanotubes were purchased from Sigma-Aldrich and Nanjing XFNANO Materials Tech Co., Ltd (XFNANO), respectively.

1.2 Synthesis of MoS$_2$ electrocatalyst under different parameters

The s-MoS$_2$ was synthesized from microwave and ultrasound-assisted method. 7 mmol sodium molybdate and 35 mmol thiourea were poured into 40 ml de-ionized (DI) water under stirring vigorously to form a mixed solution. Meanwhile, 2.0 M HCl were added to make the solution pH lower than 1 under stirring. Then the mixed solution was transferred into a 250 ml microwave-ultrasound synergistic reactor under the parameters that the reaction temperature was 200°C. The microwave power was 600 W and the ultrasonic power was 1000 W. These parameters were constant and the reaction time was set as 3, 6, 9 and 12 h. After the reaction, the samples were centrifuged, washed with DI water and alcohol, and dried at 60°C for 12 hours to obtain a MoS$_2$ electrocatalysts. The electrochemical performance was compared and a set of parameters with the best hydrogen evolution performance were selected with the reaction time was 12 h.

The m-MoS$_2$ and s-MoS$_2$ sample was prepared with taking reaction time and ultrasonic power as invariants and microwave power as variables. The prepared solution was reacted under the parameters of microwave power of 0, 200, 400, 600,

and 1000 W. After the reaction, the samples were centrifuged, washed with DI water and alcohol, dried at 60°C for 12 h to obtain m-MoS$_2$ electrocatalyst. The electrochemical performances were compared and a set of parameters with the best hydrogen evolution performance were selected which are microwave power of 800 W. Similarly, the optimal ultrasonic power was selected as the ultrasonic power of 1000 W.

1.3 Characterizations

X-ray diffraction (XRD) patterns were collected on a powder X-ray diffractometer at 40 kV and 15 mA using Cu-K radiation (λ=1.54056 Å, PANalytical X'Pert Powder diffractimeter). Transmission electron microscopy (TEM) and high resolution TEM (HRTEM) images were obtained on a JEOL JEM-2100F microscope at 200 kV. Scanning electron microscopy (SEM) images were recorded on the FEI Quanta 450 at high vacuum with an accelerating voltage of 10 kV. The field emission scanning electron microscopy (FESEM) were observed under a SUPRA-55 electron microscopy. Ex situ X-ray absorption near-edge spectra (XANES) of MoS$_2$ was obtained recorded with a grazing incidence angle of 0.3° at the Soft X-ray Microanalysis Beamline (SXRMB) of the Canadian Light Source (CLS; Saskatoon, SK, Canada), using a Si(111) double crystal monochromator, as shown in Figure 2c and d. The XANES spectra were normalized to incident photon flux and to unity at the maximum intensity of each spectrum.

1.4 Electrochemical characterization

The HER performance test of the MoS$_2$ electrocatalyst was carried out using a three-electrode system. The catalytic performance of the prepared samples for hydrogen evaluation reaction was measured with a three-electrode cell by linear sweep voltammetry (LSV) method on a computer controlled CHI 660E electrochemical workstation (CH Instruments, Inc., USA). The reference electrode was Ag/AgCl (4 mol/L) in saturated KCl solution, and the counter electrode was a graphite rod, and the working electrode was a glassy carbon (3 mm in diameter) supporting the measured materials. The measured materials (4 mg) were predispersed in the mixture solution of 100 μL 5 wt% nafion solution and 1000 μL dehydrated

ethanol by ultrasonication for 30 min. A 10 μL portion of the as-prepared ink was dropped on the surface of the glassy carbon, yielding a working electrode with a loading of 0.51 mg cm^{-2} after air-drying. For comparison, the commercial 20 wt % Pt/C was supported on the glassy carbon with the same loading. The LSV curves of different samples were recorded without solution agitation at a scan rate of 10 mV s^{-1} in 0.5 M H$_2$SO$_4$ or 1 M KOH solution that was purged with N$_2$ flow. According to the Nernst equation, it was converted into a relatively reversible hydrogen electrode with respect to the potential of the Ag/AgCl electrode, that is, $E_{RHE} = E_{Ag/AgCl} + 0.059*pH + 0.197$. Meanwhile, Scanning rate was 2 mV/s to record polarization curve. The working electrode had been scanned multiple times until the signal was stable. Definitively, we collected the polarization curve data and corrected it. In the Tafel diagram, the starting potential was determined according to the starting point of the linear region. Electrochemical AC Impedance (EIS) was used PARSTAT3000 electrochemical workstation to test under normal temperature and pressure and the measurement conditions were under the potential of corresponding overpotential at 10 mA cm^{-2}, in the frequency range of 0.1~100000HZ, with the sweep rate and amplitude of 10 mV/s and 0.01 V, respectively. The electrochemical active area was adopted CHI660E electrochemical workstation and the test was carried out under normal temperature and pressure. The test condition was to test the cyclic voltammetry curve at different scanning speeds (20, 40, 60, 80, 100, 120, and 140mV/s) in the Faraday zone. The middle current density was obtained by the potential to plot and finally the electric double layer capacitance was obtained by fitting. The stability test was used the CHI660E electrochemical workstation to test under normal temperature and pressure and obtained the i-t curve under the same bias voltage. At the same time, we took the bias voltage corresponding to the electrocatalyst at a current density of 10mA/cm^2 for chronopotentiometric test. The durability test was adopted the CHI660E electrochemical workstation to test under normal temperature and pressure and it was characterized by the deviation between the HER curve and the original curve of the catalyst after several thousand cycles of cyclic voltammetry.

Greatly different from that of h-MoS$_2$, the m-MoS$_2$ exhibits micro-spherical shape with larger diameters of ~650 nm, which are comprised of obvious nanoflakes structure with the thickness of ~20.5 nm, indicating that its product consisted of large-scale uniform nanosheets (Figure S1b). The results suggest that the "internal heating" manner with microwave heating could effectively enhance the reaction rates and the resulting MoS$_2$ has larger diameter. Nevertheless, the u-MoS$_2$ exhibits an obvious smashing morphology as shown in Figure S1c, indicating that the ultrasound could effectively provide the mechanical agitation.
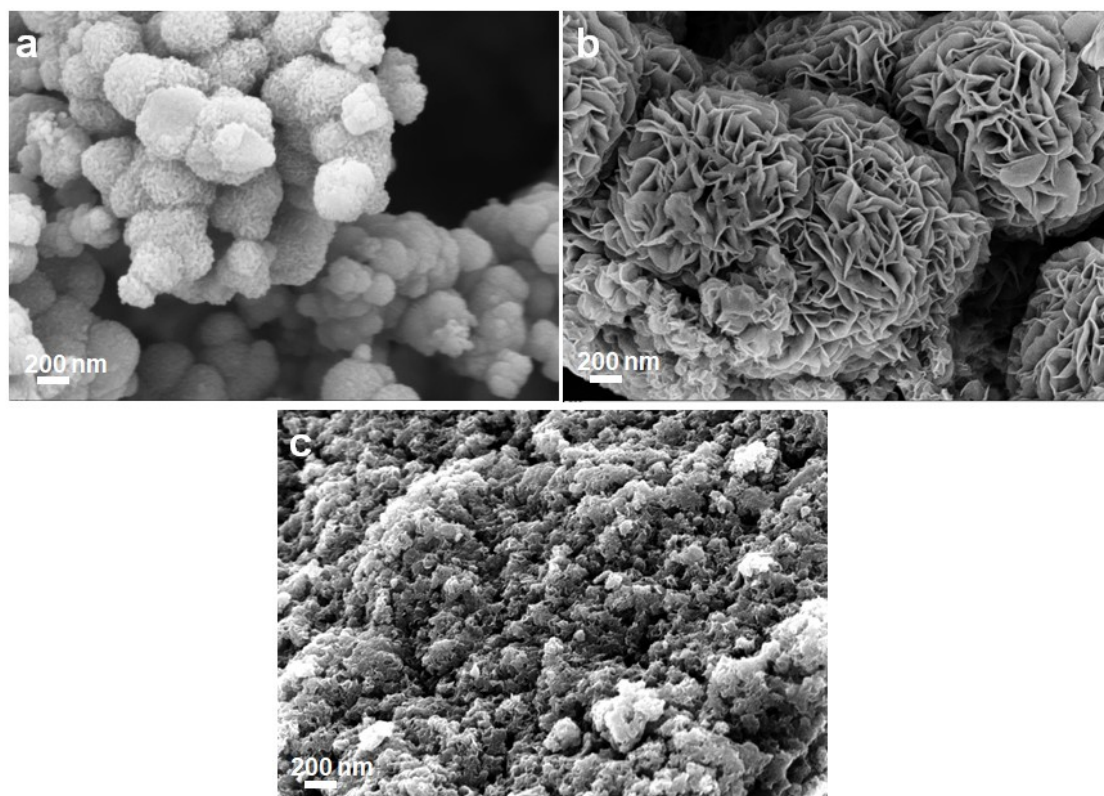
Figure S1 SEM images of a) h-MoS$_2$, b) m-MoS$_2$, and c) u-MoS$_2$, respectively.
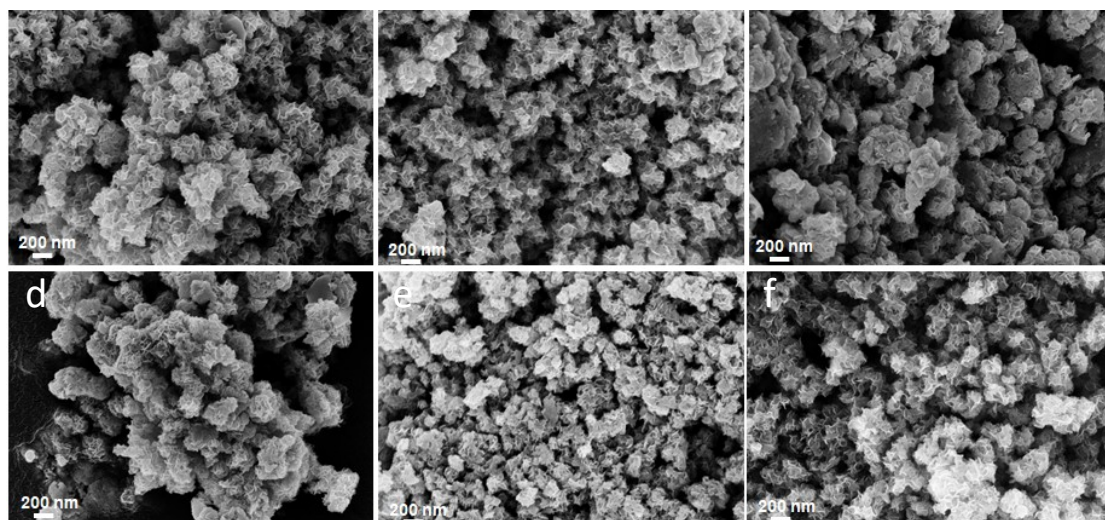
Figure S2 SEM images of u-MoS$_2$prepared with the ultrasonic power of a) 250, b) 500, c) 750, d) 1000, e) 1250, and f) 1500 W, respectively.
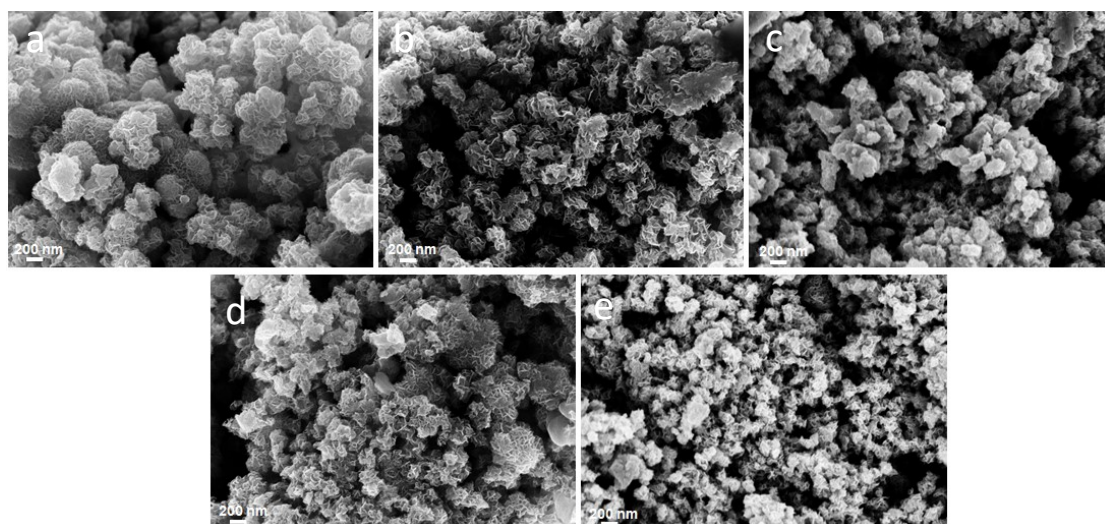

Figure S3 SEM images of m-MoS$_2$prepared with the microwave power of a) 200, b) 400, c) 600, d) 800, and f) 1000 W, respectively.
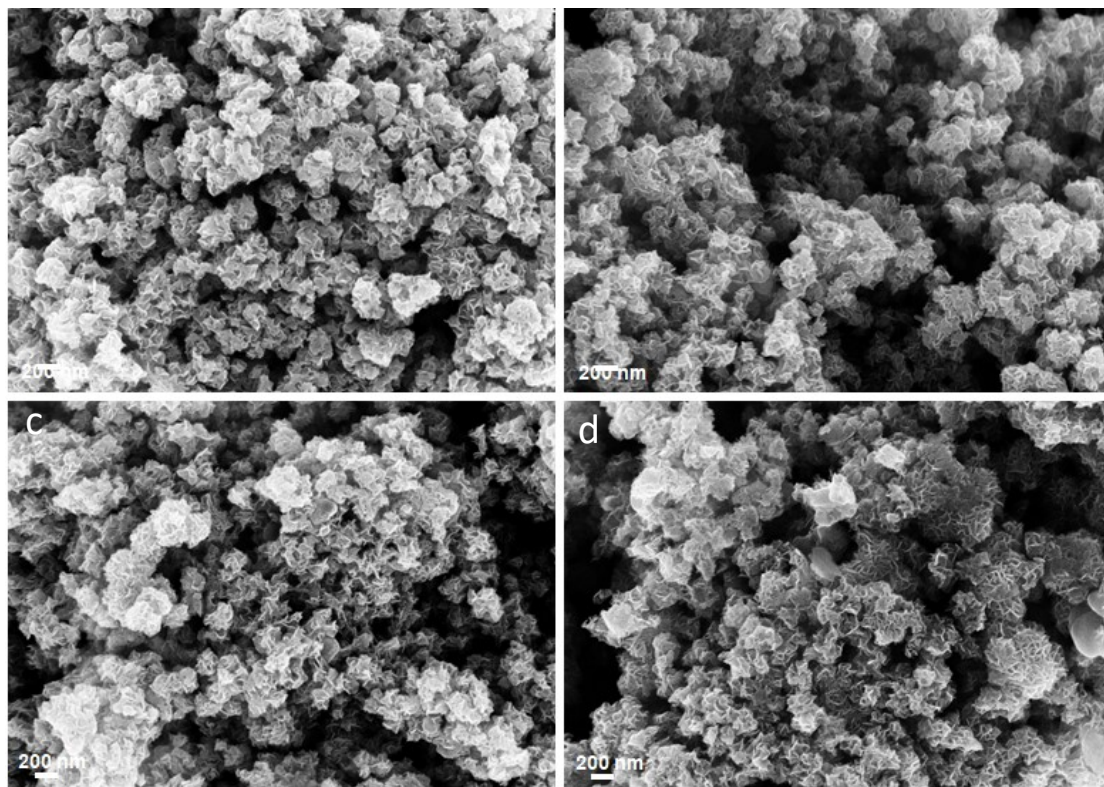
Figure S4 SEM images of s-MoS$_2$ prepared from different time, a) 3h, b) 6 h, c) 9h, and d) 12 h, with the microwave power of 800 W and ultrasonic power of 1000 W.
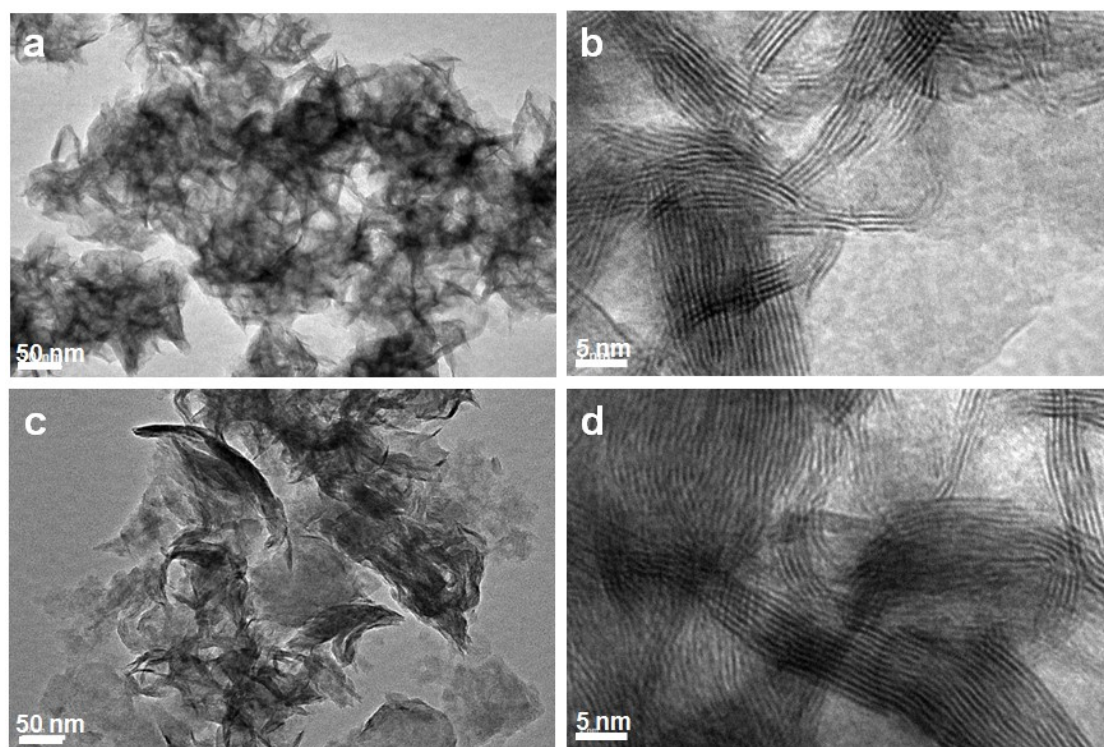

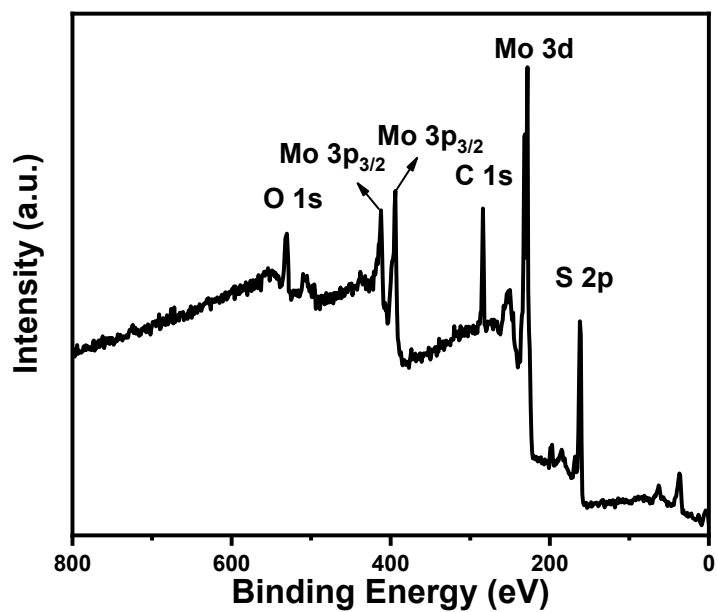Figure S5 TEM images of a,b) m-MoS$_2$ and c,d) u-MoS$_2$.
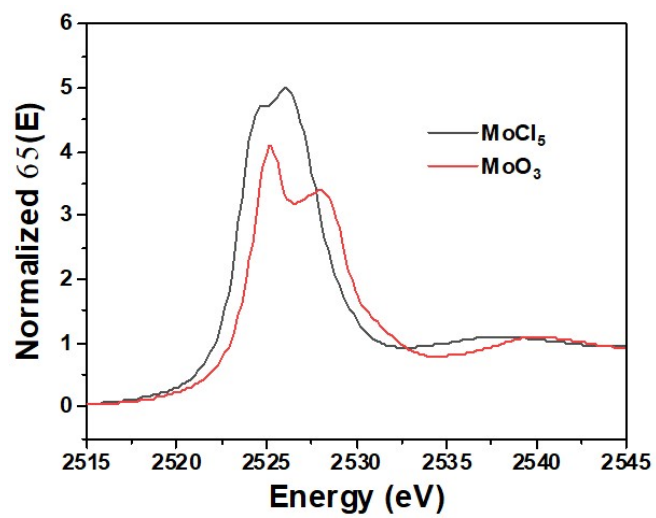
Figure S6 Survey XPS of s-MoS$_2$ sample.
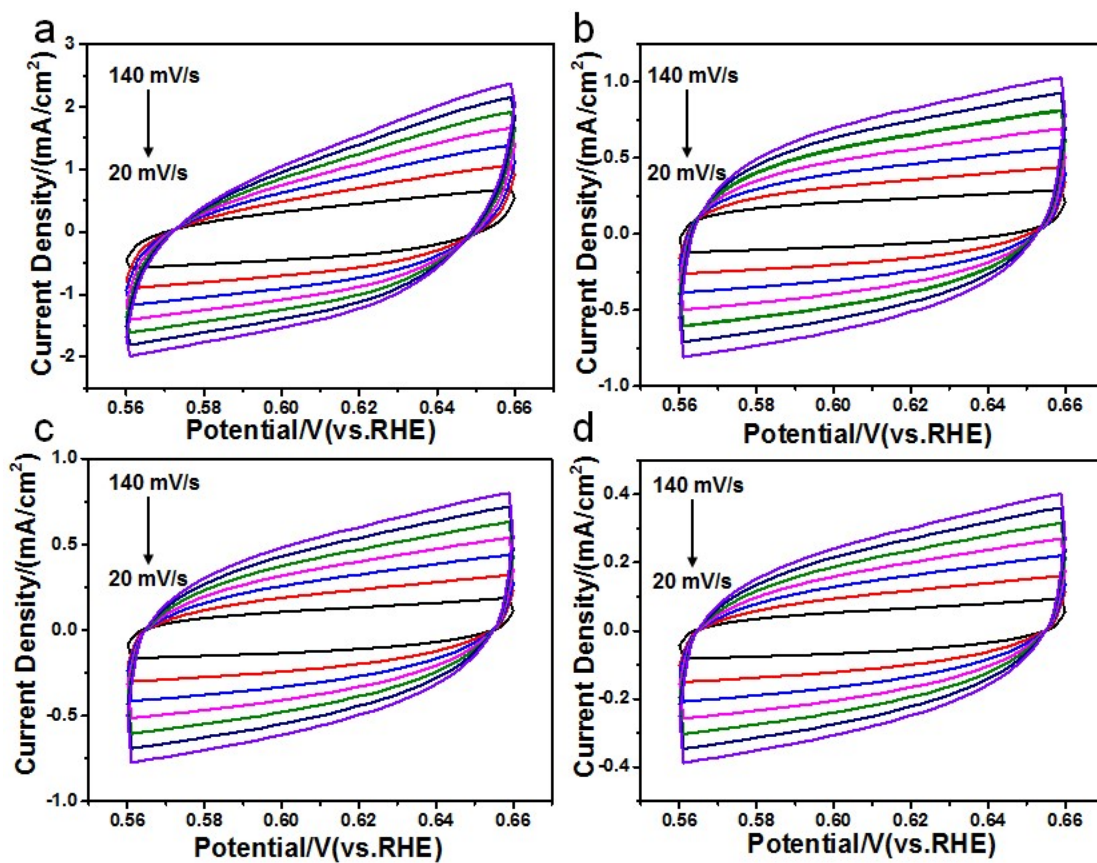

Figure S7 Mo L$_3$-edge XANES results of MoCl$_5$ and MoO$_3$.

Figure S8 Cyclic voltammetry curves in 0.5M H_2SO_4 for (a) s-MoS_2, (b) u-MoS_2, (c) m-MoS_2, and (d) h-MoS_2, respectively.
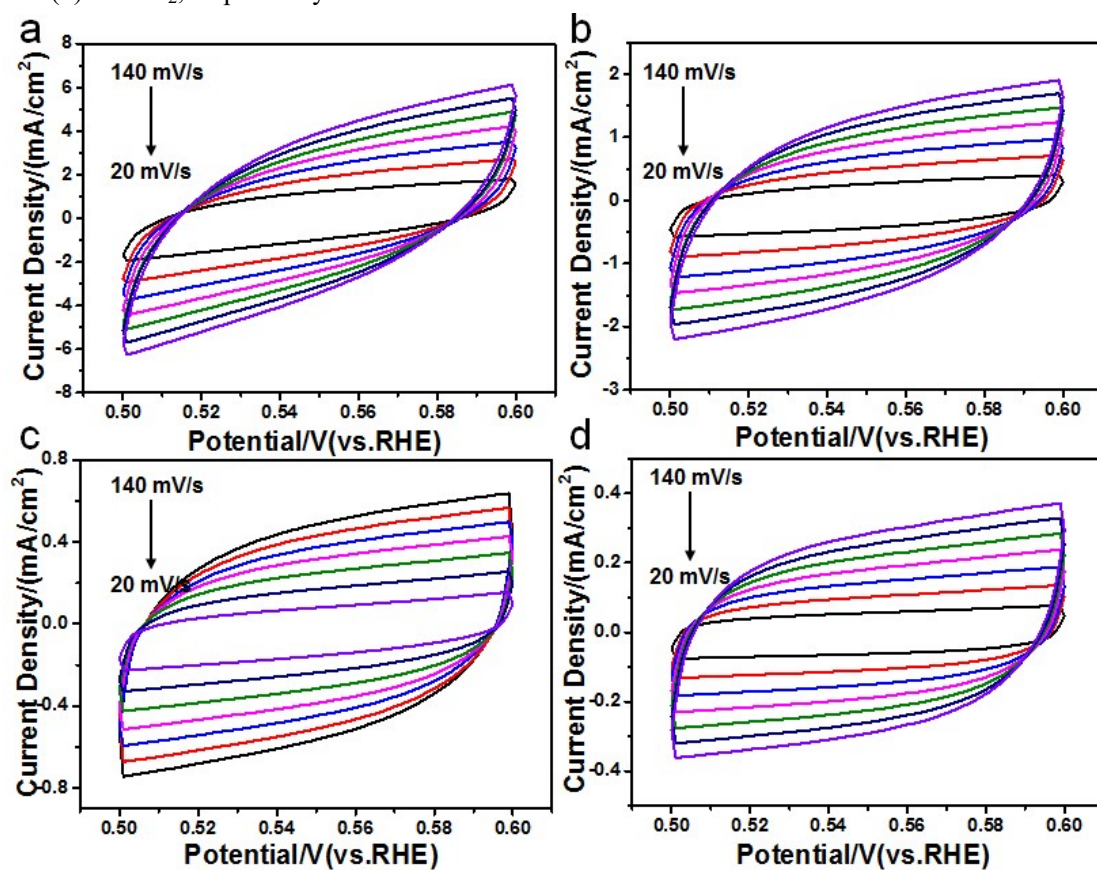
Figure S9 Cyclic voltammetry curves in 1.0 M KOH for (a) s-MoS$_2$, (b) u-MoS$_2$, (c) m-MoS$_2$, and (d) h-MoS$_2$, respectively.
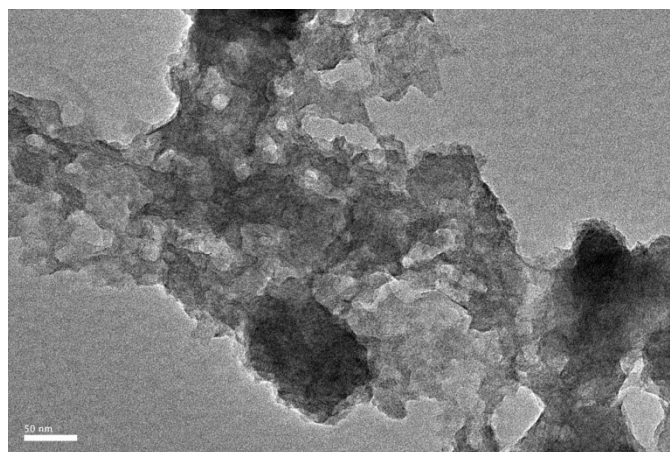

Figure S10 TEM image of s-MoS$_2$ after 20 h continuous measurement in acidic condition.

Table 1 The HER performance comparison with rep

Catalysts	Overpotential (mV) in acid/alkaline electrolyte	Tafel slope(mV/dec)in acid/alkaline electrolyte	References
s-MoS_2	175/153	61/52.5	***In this work***
MoS_2/graphene/carbonized melamine foam	163/---	76/---	Ref.1
V-MoS_2	156/---	54/---	Ref.2
MoS_2@rGO	239/---	52/---	Ref.3
Co-MoS_2/NCFCP	174/×---	52/---	Ref.4
Ni_2P/MoS_2-CC	280/170	75/95	Ref.5
Ni/MoS_2 nanosheets	---/109	---/41.2	Ref.6
g-C_3N_4/FeS_2/MoS_2	193/---	87.7/---	Ref.7
MoS_2/MoN	117/132	87/98	Ref.8
NC@Mo_2C@MoS_2	205/216	61.4/42.7	Ref.9
$Ni_{0.15}Co_{0.85}S_2$@MoS_2	---/79	---/52	Ref.10
MoS_2/FeS_2	134/---	76.8/---	Ref.11
$Co(OH)_2$/MoS_2/CC	---/101	---/28.02	Ref.12
ZnS@C@MoS_2	---/118	---/55.4	Ref.13
Co_9S_8@MoS_2/CNFs	190/---	110/---	Ref. 14
Co_9S_8/1L MoS_2	97/---	71/---	Ref. 15

1.W. Li, J. W. Chen, Z. L. Xiao, J. B. Xing, C. Yang, X. P. Qi, MoS_2/graphene/carbonized melamine foam composite catalysts for the hydrogen evolution reaction, Carbon 174 (2021) 758-758.

2.M. Y. Li, B. H. Cai, R. M. Tian, X. J. Yu, M. B. H. Breese, X. Z. Chu, Z. J. Han, S. Li, R. Joshi, A. Vinu, T. Wan, Z. M. Ao, J. B. Yi, D. W. Chu, Vanadium doped 1T MoS_2 nanosheets for highly efficient electrocatalytic hydrogen evolution in both acidic and alkaline solutions, Chem. Eng. J. 409 (2021) 128158.

3.Wang, F. Lu, K. Su, N. Zhang, Y. H. Zhang, M. Wang, X. Wang, Engineering Mo-O-C interface in MoS_2@rGO via charge transfer boosts hydrogen evolution, Chem. Eng. J. 399 (2020) 126018.

4.K. C. Wang, Z. X. Zhan, M. L. Gao, T. Lei, P. Yin, Nitrogen-doped carbon fiber/carbon paper supported Co-MoS_2 as an efficient catalyst for hydrogen evolution, Mater. Lett. 281 (2020) 128579.

5.Y. L. Xu, R. Wang, Z. Liu, L. L. Gao, T. F. Jiao, Z. F. Liu, Ni_2P/MoS_2 Interfacial Structures Loading on N-doped Carbon Matrix for Highly Efficient Hydrogen Evolution, Green Energy Environ. 2020.

6.S. Zhang, C. Fang, Y. H. Liu, S. Lin, R. Zeng, Q. L. Wei, L. S. Zeng, Y. F. Chen, B. Na, Molten salt electrolysis method to achieve Ni/MoS_2 with activity sulfur enhance the hydrogen evolution reaction performance under alkaline condition[J]. Surf.

Interfaces 21 (2020) 100789.

7. Y. Li, S. J. Zhu, Y. Xu, R. Y. Ge, J. T. Qu, M. Y. Zhu, Y. Liu, J. M. Cairney, R. K. Zheng, S. Li, J. J. Zhang, W. X. Li, FeS_2 bridging function to enhance charge transfer between MoS_2 and g-C_3N_4 for efficient hydrogen evolution reaction[J]. Chem. Eng. J. 2020 127804.

8. A. P. Wu, Y. Gu, Y. Xie, H. J. Yan, Y. Q. Jiao, D. X. Wang, C.G. Tian, Interfacial engineering of MoS_2/MoN heterostructures as efficient electrocatalyst for pH-universal hydrogen evolution reaction, J. Alloys Compd. 867 (2021) 159066.

9. L. Gong, X. Mu, Q. Li, L. Ma, Y. C. Xiong, R. Li, Rational design of Ni-induced NC @Mo_2C@MoS_2 sphere electrocatalyst for efficient hydrogen evolution reaction in acidic and alkaline media, Int. J. Hydrogen Energy 46 (2021) 5250-5258.

10. X. B. Xu, W. Zhong, L. Zhang, G. X. Liu, W. Xu, Y. W. Du, Metal organic framework derived $Ni_{0.15}Co_{0.85}S_2$@MoS_2 heterostructure as an efficient and stable electrocatalyst for hydrogen evolution, Sep. Purif. Technol. 254 (2021) 117629.

11. Y. Chen, Z. J. Peng, Y. F. Guo, S. D. Guan, X. L. Fu, Novel self-supported MoS_2/FeS_2 nanocomposite as an excellent electrocatalyst for hydrogen evolution, Solid State Sci. 101 (2020) 106156.

12. X. L. Liu, X. S. Lv, P. Wang, Q. Q. Zhang, B. B. Huang, Z. Y. Wang, Y. Y. Liu, Z. K. Zheng, Y. Dai, The synergistic effect of light irradiation and interface engineering of the $Co(OH)_2$/MoS_2 heterostructure to realize the efficient alkaline hydrogen evolution reaction, Electrochim. Acta 299 (2019) 618-625.

13. S. H. Liu, S. N. Li, K. Sekar, R. Li, Y. Y. Zhu, R. M. Xing, K. Nakata, A. Fujishima, Hierarchical ZnS@C@MoS_2 core-shell nanostructures as efficient hydrogen evolution electrocatalyst for alkaline water electrolysis, Int. J. Hydrogen Energy 44 (2019) 25310-25318.

14. H. Zhu, J. Zhang, R. Yanzhang, M. Du, Q. Wang, G. Gao, J. Wu, G. Wu, M. Zhangm B. Liu, J. Yao, X. Zhang, When Cubic Cobalt Sulfi de Meets Layered Molybdenum Disulfi de: A Core–Shell System Toward Synergetic Electrocatalytic Water Splitting, Adv. Mater. 27 (2015) 4752–4759.

15. H. Zhu, G. Gao, M. Du, J. Zhou, K. Wang, W. Wu, X. Chen, Y. Li, P. Ma, W. Dong, F. Duan, M. Chen, G. Wu, J. Wu, H. Yang, S. Guo, Atomic-Scale Core/Shell Structure Engineering Induces Precise Tensile Strain to Boost Hydrogen Evolution Catalysis, Adv. Mater. 30 (2018) 1707301.